

Reactivity and Secondary Kinetic Isotope Effects in the S_N2 Reaction Mechanism: Dioxygen Radical Anion and Related Nucleophiles

Gustavo E. Davico and Veronica M. Bierbaum*

Contribution from the Department of Chemistry and Biochemistry, University of Colorado, Boulder, Colorado 80309-0215

Received August 25, 1999

Abstract: We have measured the rate constants for the reactions of O₂^{•-} and several related anions and radical anions with alkyl halides. The results suggest that O₂^{•-} reacts with alkyl halides more rapidly than anticipated, based on anion basicities as well as on results from ab initio calculations. In addition, deuterated neutrals were used and the kinetic isotope effects (KIE) determined. These values were also calculated by using ab initio calculations and transition state theory. The agreement between experiment and theory is excellent, except for O₂^{•-} indicating that this reaction proceeds by a different reaction mechanism. We discuss competition between electron transfer and substitution mechanisms to explain the observed remarkable nucleophilicity of O₂^{•-}. A detailed analysis of the different contributions to the calculated KIEs shows that the total value is primarily determined by the C–H stretching and the CH₃ out-of-plane bending modes. The former factor is very inverse ($k_H/k_D < 1$), and it does not change significantly for different reactions. However, the bending factor changes markedly from one reaction to another and therefore becomes the factor that determines how the total KIEs change for different reactions. As a result, the KIEs are related to the *crowdedness* of the transition states. This effect is discussed in detail with respect to the conventional *looseness* interpretation.

Introduction

The S_N2 mechanism¹ has been extensively studied in both the gas phase and condensed phase; however, many important questions remain. This mechanism continues to be the target of experimental^{2–6} and theoretical^{7–12} studies because it plays a fundamental role in organic chemistry and represents a prototypical displacement reaction.

The dioxygen radical anion, O₂^{•-}, commonly referred to as superoxide anion, has been recognized by McDonald et al. as a “super S_N2 nucleophile” due to its high reaction efficiency with common S_N2 substrates such as methyl chloride or methyl bromide.¹³ In addition, electron transfer (ET) reactions of O₂^{•-} have been reported in cases where the substrates are very efficient electron acceptors; for these reactions, electron transfer

can be distinguished from the S_N2 channel, as in polyhalogenated hydrocarbons^{5,14,15} and perfluoroketones.¹³ From these results, the question of which mechanism (S_N2 or ET) operates in the reactions of O₂^{•-} with alkyl halides clearly emerges.

Kinetic isotope effects (KIE) have shed light on many aspects of the S_N2 reaction ranging from solvation effects to transition state (TS) compression in enzymes.^{2,16–30} Theoretical studies have been extremely helpful to further understand these processes. Secondary α-deuterium KIEs have been used to

* Corresponding author. E-mail: Veronica.Bierbaum@Colorado.edu. Fax: (303) 492-5894.

(1) Shaik, S. S.; Schlegel, H. B.; Wolfe, S. *Theoretical Aspects of Physical Organic Chemistry. The S_N2 Mechanism*; Wiley: New York, 1992.

(2) Gronert, S.; DePuy, C. H.; Bierbaum, V. M. *J. Am. Chem. Soc.* **1991**, *113*, 4009–10.

(3) Viggiano, A. A.; Arnold, S. T.; Morris, R. A.; Ahrens, A. F.; Hierl, P. M. *J. Phys. Chem.* **1996**, *100*, 14397–14402.

(4) DePuy, C. H.; Gronert, S.; Mullin, A.; Bierbaum, V. M. *J. Am. Chem. Soc.* **1990**, *112*, 8650.

(5) Staneke, P. O.; Groothuis, G.; Ingemann, S.; Nibbering, N. M. M. *J. Phys. Org. Chem.* **1996**, *9*, 471–486.

(6) Wilbur, J. L.; Brauman, J. I. *J. Am. Chem. Soc.* **1991**, *113*, 9699.

(7) Dewar, M. J. S.; Yuan, Y. C. *J. Am. Chem. Soc.* **1990**, *112*, 2095–105.

(8) Sastry, G. N.; Shaik, S. *J. Phys. Chem.* **1996**, *100*, 12241–12252.

(9) Sastry, G. N.; Danovich, D.; Shaik, S. *Angew. Chem., Int. Ed. Engl.* **1996**, *35*, 1098–1100.

(10) Sastry, G. N.; Shaik, S. *J. Am. Chem. Soc.* **1995**, *117*, 3290–3291.

(11) Shaik, S. *Acta Chem. Scand.* **1990**, *44*, 205.

(12) Glukhovtsev, M. N.; Pross, A.; Radom, L. *J. Am. Chem. Soc.* **1995**, *117*, 2024.

(13) McDonald, R. L.; Chowdhury, A. K. *J. Am. Chem. Soc.* **1985**, *107*, 4123.

(14) Mayhew, C. A.; Peverall, R.; Watts, P. *Int. J. Mass Spectrom. Ion Processes* **1993**, *125*, 81.

(15) Streit, G. E. *J. Phys. Chem.* **1982**, *86*, 2321.

(16) Hu, W.-P.; Truhlar, D. G. *J. Am. Chem. Soc.* **1994**, *116*, 7797–800.

(17) O’Hair, R. A. J.; Davico, G. E.; Hacaloglu, J.; Dang, T. T.; DePuy, C. H.; Bierbaum, V. M. *J. Am. Chem. Soc.* **1994**, *116*, 3609–10.

(18) Poirier, R. A.; Wang, Y.; Westaway, K. C. *J. Am. Chem. Soc.* **1994**, *116*, 2526–33.

(19) Boyd, R. J.; Kim, C. K.; Shi, Z.; Weinberg, N.; Wolfe, S. *J. Am. Chem. Soc.* **1993**, *115*, 10147–52.

(20) Zhao, X. G.; Lu, D. H.; Liu, Y. P.; Lynch, G. C.; Truhlar, D. G. *J. Chem. Phys.* **1992**, *97*, 6369–83.

(21) Zhao, X. G.; Tucker, S. C.; Truhlar, D. G. *J. Am. Chem. Soc.* **1991**, *113*, 826–32.

(22) Viggiano, A. A.; Paschkewitz, J.; Morris, R. A.; Paulson, J. F.; Gonzalez-Lafont, A.; Truhlar, D. G. *J. Am. Chem. Soc.* **1991**, *113*, 9404–5.

(23) Tucker, S. C.; Truhlar, D. G. *J. Am. Chem. Soc.* **1990**, *112*, 3338–47.

(24) Mihel, I.; Knipe, J. O.; Coward, J. K.; Schowen, R. L. *J. Am. Chem. Soc.* **1979**, *101*, 4349.

(25) Gray, C. H.; Coward, J. K.; Schowen, K. B.; Schowen, R. L. *J. Am. Chem. Soc.* **1979**, *101*, 4351.

(26) Hegazi, M. F.; Borchardt, R. T.; Schowen, R. L. *J. Am. Chem. Soc.* **1979**, *101*, 4359.

(27) Rodgers, J.; Femec, D. A.; Schowen, R. L. *J. Am. Chem. Soc.* **1982**, *104*, 3263.

(28) Wolfe, S.; Kim, C. K. *J. Am. Chem. Soc.* **1991**, *113*, 8056.

(29) Glad, S. S.; Jensen, F. *J. Am. Chem. Soc.* **1997**, *119*, 227.

(30) Hu, W. P.; Truhlar, D. G. *J. Am. Chem. Soc.* **1995**, *117*, 10726.

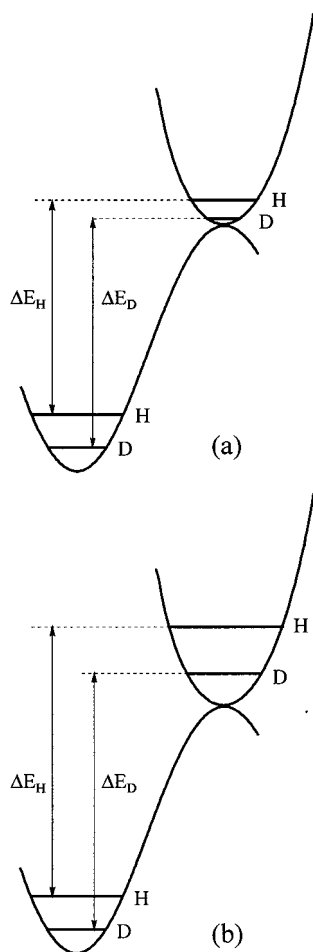


Figure 1. Schematic diagrams of potential energy surfaces indicating the activation barriers for hydrogen and deuterium labeled compounds: (a) normal KIE, $\Delta E_H < \Delta E_D$ and $k_H/k_D > 1$; (b) inverse KIE, $\Delta E_H > \Delta E_D$ and $k_H/k_D < 1$.

determine the transition state structures in S_N2 reactions.³¹ It has been recognized that a “normal” KIE ($k_H/k_D > 1$) will be associated with a reaction where the zero point energy (ZPE) difference between the protio and the deuterated structures is smaller in the transition states than in the reactants (Figure 1a). As Figure 1 also illustrates, the “inverse” KIE ($k_H/k_D < 1$) is related to a larger ZPE difference in the transition states relative to reactants. But, as Truhlar has shown in a series of papers, this picture is incomplete because there are not only vibrations but also translations and rotations that contribute to the total KIE.^{16,20–22} Recently, there has been considerable controversy concerning the kinds of frequencies involved in determining the ZPE changes shown in Figure 1 and how they relate to the TS structure.^{18,19,28,29} We will discuss this issue in light of our experimental and ab initio results.

In this paper we report the experimental rate constants for reactions of $O_2^{\bullet-}$ and several anions and radical anions of similar basicity with a variety of halogenated hydrocarbons. In addition, we report both experimental α -H(D) KIEs as well as values calculated with high level ab initio methods as a tool to probe the mechanism of these reactions.

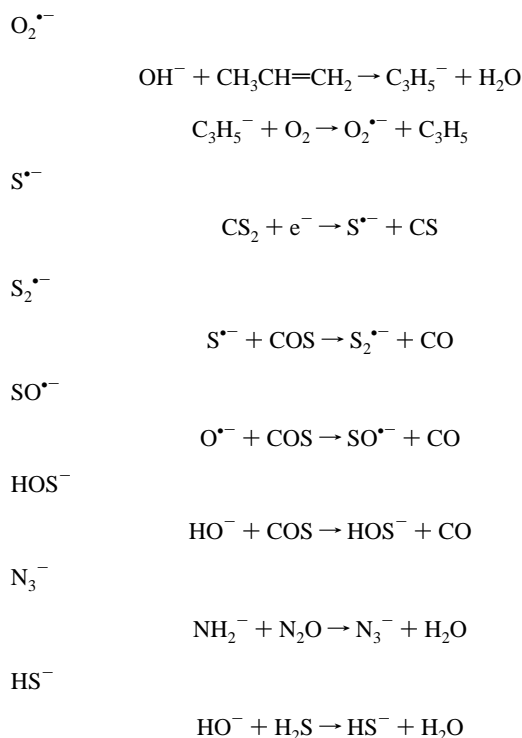
Experimental Section

All experiments were carried out with a tandem flowing afterglow-selected ion flow tube instrument (FA-SIFT) that has been described

(31) Matsson, O.; Westaway, K. C. *Adv. Phys. Org. Chem.* **1998**, *31*, 143–248 and references therein.

in detail previously.³² Ions are prepared in a rapidly flowing stream of helium buffer gas by electron impact on a suitable neutral precursor or by reactions between primary reagent ions (such as OH^- or NH_2^-) and neutral reagents that are added downstream. At the end of this flow tube, the gases are removed by a roots pump while the ions are sampled through a 2 mm orifice into a differentially pumped selection region where they are focused into a quadrupole mass filter via a series of electrostatic lenses. Tuning the quadrupole to transmit only ions of a certain m/z allows selection of the reactant ions of interest. The mass-selected ions are injected into a second flow tube, where they are entrained in helium buffer gas. The ions in this reaction flow tube undergo multiple collisions with helium and are rapidly thermalized to room temperature before being allowed to react with the neutral reagent. Ions are then sampled into the detection region where they are separated by a second quadrupole mass filter and counted with an electron multiplier. Reaction rate coefficients can be measured by introducing the neutral reagent at different positions along the reaction flow tube and monitoring the intensity of the reactant ion as a function of this reaction distance.

Ions were generated by the following reactions:



Rate constants for reaction of ions with the perprotio and perdeuterio neutral reactants were determined one after the other on the same day. Each reported rate constant value represents the average of at least three measurements carried out at 300 ± 1 K. Reported errors in the rate constants represent one standard deviation, and appropriate propagation of errors was applied to estimate errors in the KIEs. Helium, 99.995%, was purified by passage through a molecular sieve trap at 77 K. Reagents were obtained from commercial sources and were purified by using molecular sieves and by several freeze–pump–thaw cycles before use.

Molecular orbital calculations were performed using the Gaussian 92 suite of programs.³³ Structures were fully optimized at the MP2/6-31++G** level (i.e., double split valence basis set with polarization and diffuse functions on all atoms and Møller–Plesset (MP) perturba-

(32) Van Doren, J. M.; Barlow, S. E.; DePuy, C. H.; Bierbaum, V. M. *Int. J. Mass Spectrom. Ion Processes* **1987**, *81*, 85.

(33) Frisch, M. J.; Trucks, G. W.; Head-Gordon, M.; Gill, P. M.; Wong, M. W.; Foresman, J. B.; Johnson, B. G.; Schlegel, H. B.; Robb, M. A.; Replogle, E. S.; Gomperts, R.; Andres, J. L.; Raghavachari, K.; Binkley, J. S.; Gonzales, C.; Martin, R. L.; Fox, D. J.; Defrees, D. J.; Baker, J.; Stewart, J. J. P.; Pople, J. A. *Gaussian 92, Revision C*; Gaussian, Inc.: Pittsburgh, PA, 1992.

tion theory to second order³⁴) using the standard gradient geometry optimization method; the only constraint was maintaining the symmetries specified. Final relative energies were obtained by single-point MP4(SDTQ)/6-31++G** calculations on the MP2/6-31++G** geometries (MP4(SDTQ)/6-31++G**//MP2/6-31++G**). In all cases we did not correlate the core electrons, and calculations on systems with an even number of electrons were spin restricted while those on systems with an odd number of electrons were spin unrestricted.

Vibrational frequency calculations at the MP2/6-31++G** level were used to characterize all stationary points as either minima (zero imaginary frequency) or first-order saddle points (single imaginary frequency). The intrinsic reaction coordinate (IRC) technique in internal mass-weighted coordinates^{35,36} was used to confirm that transition states connect the corresponding minima on either side. Spin contamination in the open shell species was found to be very small, with $\langle S^2 \rangle$ values ranging from 0.75 to 0.78.

Using transition state theory³⁷ the total KIE (η) can be calculated as

$$\eta = \frac{k_H}{k_D} = \frac{Q_H^{\text{TS}}/Q_H^{\text{R}}}{Q_D^{\text{TS}}/Q_D^{\text{R}}} e^{-\Delta\Delta E/k_B T} \quad (1)$$

where Q 's are the total partition functions with subscripts indicating isotopic substitution and superscripts indicating reactants (R) or transition state (TS). k_B is Boltzmann's constant, T is the temperature, and $\Delta\Delta E$ is the difference in the potential energy difference between the transition state and reactants for the perprotio and the perdeuterio labeled reaction. Since we calculate the vibrational partition function with the zero of energy at the classical well instead of at $\nu = 0$, $\Delta\Delta E$ becomes zero. Noting that each total partition function is the product of a translational, a rotational, and a vibrational partition function, we can write

$$\eta = \eta_{\text{trans}}\eta_{\text{rot}}\eta_{\text{vib}} \quad (2)$$

where the terms represent the translational, rotational, and vibrational contributions, respectively, to the total isotope effect. To achieve a more detailed understanding, we further factor η_{vib} into contributions from groups of frequencies:

$$\eta_{\text{vib}} = \prod_n \eta_{\text{vib}}^n \quad (3)$$

Here n is the total number of groups.

Rotational partition functions were calculated classically from moments of inertia determined from MP2/6-31++G** geometries for both reactants and transition states. Harmonic frequencies (not scaled) obtained at the same level were used to calculate the vibrational partition functions by using a custom program that also calculates the contributions of each predefined group of frequencies to the vibrational KIE. The definition of the number of groups and the method of grouping can be arbitrary. Some authors arrange groups by the frequency values,^{16,20–22} while others choose a collection of specific frequencies for analysis and gather the rest together.¹⁸ We employed a different approach and grouped the frequencies by their physical significance; this method allows us to analyze the nature of the KIEs in a more detailed way. However, this approach is time-consuming and includes analysis and animation of each frequency for each of the minima and transition states for all the reactions studied, including isotopically labeled reactions. This was achieved, in part, by using the program *Gaussview*. All the frequencies were then included in one of the following groups: η_{low} , frequencies that are converted from rotational and translational modes in reactants to vibrational modes in the transition states; $\eta_{\text{str,C-X}}$, stretching frequency between the carbon atom and the leaving group; $\eta_{\text{str,C-H}}$, C–H stretching modes; η_{Nuis} , internal modes in the nucleophile (only for polyatomic nucleophiles); $\eta_{\text{ben,out}}$,

out-of-plane bending modes in the CH_3 moiety; $\eta_{\text{ben,in}}$, in-plane bending modes in the CH_3 moiety (scissors).

We did not include tunneling effects since they have been shown to have a minor or negligible influence on the KIEs for this type of reaction.^{16,20} All calculations were carried out for $T = 300$ K.

Results and Discussion

Reactivity. Table 1 shows the experimental rate constants for $\text{O}_2^{\bullet-}$ and for several nucleophiles of similar basicity including oxygen-, sulfur-, and nitrogen-centered nucleophiles reacting with a variety of alkyl halides. Some of these ions are closed-shell species while others are radical anions. The unusually high reactivity of $\text{O}_2^{\bullet-}$ with respect to ions of similar basicity is clearly evident in the table. For example, $\text{O}_2^{\bullet-}$ reacts with methyl chloride at a rate 10 times faster than does HOS^- , which has the same basicity within experimental error.

Figure 2 shows a plot of reaction efficiencies for $\text{S}_{\text{N}}2$ reactions with methyl chloride versus basicity of the nucleophile. From this plot it is clear that the reaction efficiency of $\text{O}_2^{\bullet-}$ is comparable to that of nucleophiles that are 15 kcal/mol more basic, and this efficiency is 1 order of magnitude greater than those of nucleophiles of similar basicity. However, other radical anions (e.g., $\text{S}^{\bullet-}$, $\text{SO}^{\bullet-}$) have rates comparable to those observed for closed-shell species of similar basicities; this suggests that the origin of the enhanced reactivity of $\text{O}_2^{\bullet-}$ is not its radical character. In contrast, it has been shown that radical anions react less efficiently than related anions in $\text{S}_{\text{N}}2$ reactions.³⁸ Moreover, the enhanced reactivity is not due to the localization of charge on oxygen since other oxygen-centered nucleophiles do not show this behavior, as can be seen in Figure 2.

Similar conclusions can be drawn for methyl bromide as a neutral reagent (Table 1). However, in these cases the reactions are faster and the differences in reactivity between $\text{O}_2^{\bullet-}$ and the other nucleophiles are less pronounced.

As discussed previously and confirmed by these results, there is no apparent difference in the nucleophilicity of oxygen and sulfur centered nucleophiles. This indicates that the enhanced reactivity of sulfur nucleophiles in the condensed phase has its origin in solvent effects.^{4,39}

Analysis of the rates obtained for branched alkyl halides is more complicated since elimination is now possible; since the ionic products of elimination and substitution are the same, we cannot distinguish between these mechanisms. Nevertheless, consider the reactivity of methyl chloride and ethyl chloride with HOS^- and $\text{O}_2^{\bullet-}$. Although these nucleophiles have the same basicity that is sufficient for the elimination reaction to be exothermic ($\Delta H_{\text{acid}} > 351$ kcal/mol⁴⁰), the reactivity of HOS^- decreases about 1 order of magnitude in going from methyl to ethyl chloride while the reactivity of $\text{O}_2^{\bullet-}$ increases. This is consistent with our earlier work that demonstrated that when elimination is thermodynamically allowed, sulfur-centered nucleophiles exhibit less facile elimination reactions than do oxygen-centered nucleophiles.² An intriguing feature is that other oxygen-centered nucleophiles with similar basicities (e.g., $\text{C}_2\text{F}_5\text{CH}_2\text{O}^-$, which is slightly more basic than $\text{O}_2^{\bullet-}$ with $\Delta H_{\text{acid}}(\text{C}_2\text{F}_5\text{CH}_2\text{OH}) = 357$ kcal/mol) also show a decrease in the rate when going from methyl to ethyl chloride.⁴ However, the reactivity of $\text{O}_2^{\bullet-}$ continues to increase for reaction with

(38) Born, M.; Ingemann, S.; Nibbering, N. M. M. *Mass Spectrom. Rev.* **1997**, *16*, 181–200.

(39) Olmstead, W. N.; Brauman, J. I. *J. Am. Chem. Soc.* **1977**, *99*, 4219.

(40) *NIST Chemistry WebBook, NIST Standard Reference Database Number 69*; Mallard, W. G., Linstrom, P. J., Eds.; National Institute of Standards and Technology: Gaithersburg MD, 1998 (<http://webbook.nist.gov>).

(34) Hehre, W. J.; Radom, L.; Schleyer, P. R.; Pople, J. A. *Ab Initio Molecular Orbital Theory*; Wiley: New York, 1986.

(35) Gonzalez, C.; Schlegel, H. B. *J. Phys. Chem.* **1990**, *94*, 5523.

(36) Gonzalez, C.; Schlegel, H. B. *J. Chem. Phys.* **1989**, *90*, 2154.

(37) Eyring, H. *J. Chem. Phys.* **1935**, *3*, 107.

Table 1. Experimental Rate Constants^a and Kinetic Isotope Effects

$\Delta H_{\text{acid}}^{\text{AH}}$ EA(A)	nucleophile ^b (A ⁻)						
	O ₂ ⁻ 355 kcal/mol ^c 0.451 eV	HOS ⁻ 354 kcal/mol ^d 1.657 eV ^d	S ⁻ 351 kcal/mol 2.077 eV	HS ⁻ 351 kcal/mol 2.317 eV	SO ⁻ 348 kcal/mol 1.125 eV	N ₃ ⁻ 344 kcal/mol 2.762 eV	S ₂ ⁻ 331 kcal/mol 1.670 eV
CH ₃ Cl	(6.33 ± 0.04) × 10 ⁻¹⁰	(6.72 ± 0.07) × 10 ⁻¹¹	(4.25 ± 0.08) × 10 ⁻¹¹	(1.31 ± 0.03) × 10 ⁻¹¹	(6.71 ± 0.01) × 10 ⁻¹¹	(7.37 ± 0.03) × 10 ⁻¹²	(3.43 ± 0.03) × 10 ⁻¹¹
CD ₃ Cl	(6.96 ± 0.07) × 10 ⁻¹⁰	(7.00 ± 0.10) × 10 ⁻¹¹	(4.42 ± 0.02) × 10 ⁻¹¹	(1.24 ± 0.02) × 10 ⁻¹¹	(6.80 ± 0.09) × 10 ⁻¹¹	(7.97 ± 0.10) × 10 ⁻¹²	(3.48 ± 0.03) × 10 ⁻¹¹
<i>k_{H/D}</i>	0.91 ± 0.01	0.96 ± 0.02	0.96 ± 0.02	1.06 ± 0.03	0.98 ± 0.02	0.92 ± 0.01	0.99 ± 0.01
CH ₃ CH ₂ Cl	(8.21 ± 0.06) × 10 ⁻¹⁰	(7.51 ± 0.08) × 10 ⁻¹²	(1.31 ± 0.01) × 10 ⁻¹²		(2.24 ± 0.01) × 10 ⁻¹¹		(9.34 ± 0.10) × 10 ⁻¹²
(CH ₃) ₂ CHCl	(8.87 ± 0.05) × 10 ⁻¹⁰				<10 ⁻¹²		<10 ⁻¹²
(CH ₃) ₃ CCl	(4.40 ± 0.04) × 10 ⁻¹⁰						
(CD ₃) ₃ CCl	(4.15 ± 0.04) × 10 ⁻¹⁰						
<i>k_{H/D}</i>	1.06 ± 0.01						
(CH ₃) ₂ CCH ₂ Cl	(7.31 ± 0.15) × 10 ⁻¹¹ ^e						
CH ₃ Br	(1.224 ± 0.005) × 10 ⁻⁹	(5.46 ± 0.04) × 10 ⁻¹⁰	(4.67 ± 0.02) × 10 ⁻¹⁰		(5.83 ± 0.10) × 10 ⁻¹⁰		(3.43 ± 0.03) × 10 ⁻¹¹
CD ₃ Br	(1.266 ± 0.006) × 10 ⁻⁹	(5.60 ± 0.02) × 10 ⁻¹⁰	(4.98 ± 0.03) × 10 ⁻¹⁰		(6.16 ± 0.02) × 10 ⁻¹⁰		(3.48 ± 0.03) × 10 ⁻¹¹
<i>k_{H/D}</i>	0.97 ± 0.01	0.98 ± 0.01	0.94 ± 0.01		0.95 ± 0.02		0.99 ± 0.01
CH ₃ CH ₂ Br	(1.70 ± 0.03) × 10 ⁻⁹	(5.19 ± 0.01) × 10 ⁻¹⁰	(4.21 ± 0.02) × 10 ⁻¹⁰		(6.50 ± 0.05) × 10 ⁻¹⁰		(9.34 ± 0.10) × 10 ⁻¹²
(CH ₃) ₂ CHBr	(1.85 ± 0.04) × 10 ⁻⁹	(1.09 ± 0.01) × 10 ⁻¹⁰	(2.67 ± 0.03) × 10 ⁻¹¹		(3.49 ± 0.01) × 10 ⁻¹⁰		<10 ⁻¹²
(CD ₃) ₂ CDBr	(1.82 ± 0.01) × 10 ⁻⁹	(1.04 ± 0.03) × 10 ⁻¹⁰	(1.21 ± 0.03)		(2.21 ± 0.05) × 10 ⁻¹⁰		
<i>k_{H/D}</i>	1.02 ± 0.02	1.05 ± 0.03	1.21 ± 0.03		1.02 ± 0.02		
(CH ₃) ₃ CBr	(1.68 ± 0.02) × 10 ⁻⁹		(1.64 ± 0.02) × 10 ⁻¹¹		(1.96 ± 0.06) × 10 ⁻¹¹ ^e		
c-(CH ₂) ₂ CHBr	(1.47 ± 0.04) × 10 ⁻¹⁰		(3.47 ± 0.10) × 10 ⁻¹²				
CH ₃ I		(8.91 ± 0.05) × 10 ⁻¹⁰	(9.27 ± 0.19) × 10 ⁻¹⁰		(9.48 ± 0.03) × 10 ⁻¹⁰		(2.39 ± 0.04) × 10 ⁻¹⁰
CD ₃ I		(8.85 ± 0.03) × 10 ⁻¹⁰	(9.61 ± 0.10) × 10 ⁻¹⁰		(9.70 ± 0.03) × 10 ⁻¹⁰		(2.44 ± 0.04) × 10 ⁻¹⁰
<i>k_{H/D}</i>		1.01 ± 0.01	0.96 ± 0.02		0.98 ± 0.01		0.98 ± 0.02

^a Rate constants in cm³ molecule⁻¹ s⁻¹. ^b Acidities and electron affinities taken from ref 40 unless otherwise stated. ^c From ref 13. ^d From ref 41. ^e Formation of adduct was also observed. The rate constant was adjusted by the amount of adduct formed, corrected for mass discrimination.

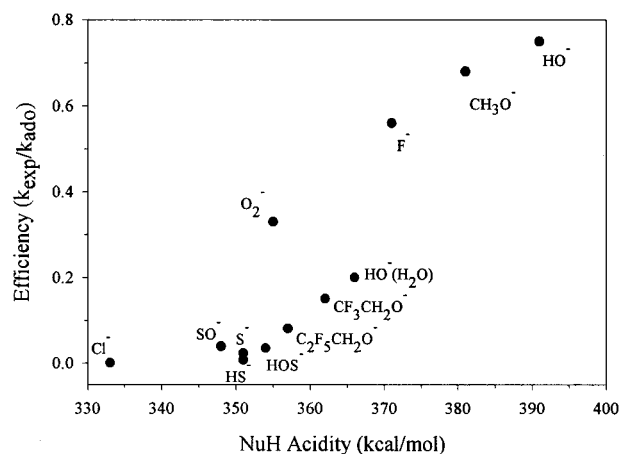


Figure 2. Dependence of the efficiency ($k_{\text{exp}}/k_{\text{ADO}}$) for the reaction $\text{Nu}^- + \text{CH}_3\text{Cl}$ with respect to the acidity of the nucleophile conjugate acid. Experimental data from this work and refs 2, 4, 17, and 53.

the more highly branched isopropyl chloride; this feature is seen only for much more basic nucleophiles (with conjugate acidity values higher than 362 kcal/mol), where elimination is very exothermic.⁴ Similar behavior is observed with the bromide series, but in this case elimination reactions are exothermic for nucleophiles with conjugate acidity values of 343 kcal/mol or higher.⁴⁰

An especially interesting case is $\text{SO}^{\cdot-}$. This ion shows a rate decrease in going from methyl chloride to ethyl chloride because elimination through the oxygen or the sulfur atom is expected to be slightly endothermic.⁴⁰ However, for the bromide series, $\text{SO}^{\cdot-}$ shows increasing reactivity when going from methyl bromide to ethyl bromide, whereas other sulfur-centered nucleophiles of similar basicity (for example $\text{S}^{\cdot-}$ and HS^-) show decreasing reactivity.⁴ This behavior led us to conclude that $\text{SO}^{\cdot-}$ is undergoing elimination reactions at the oxygen atom, which is favored kinetically, even though this path is about 5 kcal/mol less exothermic than elimination at the sulfur atom.⁴¹

To understand the factors that govern the reactivity of $\text{O}_2^{\cdot-}$ and the origin of its supernucleophilicity, we performed ab initio calculations. Table 2 shows the computed reaction energies, as well as experimental reaction enthalpies for comparison, for methyl chloride as a neutral reactant and for a set of nucleophiles including $\text{O}_2^{\cdot-}$, related anions, and other well-studied nucleophiles as references. The excellent agreement between the calculated and the experimental values suggests that calculations at this level give reasonable energies, including those that involve open-shell species, where experimental values are available. Table 2 also gives the calculated activation energies. These barriers correlate nicely with the reaction rates measured experimentally; an increase in the barrier corresponds to a decrease in the rate and vice-versa, *except for* $\text{O}_2^{\cdot-}$. According to the calculated values, $\text{O}_2^{\cdot-}$ should react with methyl chloride at a rate slightly slower than that for the $\text{OH}^- + \text{CH}_3\text{F}$ reaction; in fact the $\text{O}_2^{\cdot-} + \text{CH}_3\text{Cl}$ reaction is more than 1 order of magnitude faster.

Similar conclusions can be drawn by comparing $\text{O}_2^{\cdot-}$ and $\text{SO}^{\cdot-}$. This latter radical anion can in principle react at either the oxygen atom ($\text{SO}^{\cdot-}$) or the sulfur atom ($\text{OS}^{\cdot-}$). Even when the latter involves a more exothermic reaction, the former is kinetically favored. According to these results $\text{SO}^{\cdot-}$ and $\text{O}_2^{\cdot-}$ should react at approximately the same rate, but in fact $\text{O}_2^{\cdot-}$

(41) O'Hair, R. A. J.; DePuy, C. H.; Bierbaum, V. M. *J. Phys. Chem.* 1993, 97, 7955.

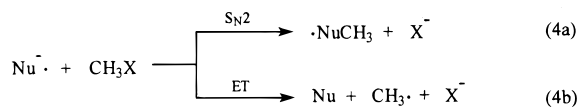
Table 2. Stationary Point Energies (kcal/mol), Relative to Reactants^a

reaction ^b	ΔE_{TS}	ΔE_{r}	$\Delta H_{\text{f}}(\text{expt})$
$\text{F}^- + \text{CH}_3\text{Cl}$	-10.4	-27.4	-30.95 \pm 0.01
$\text{Cl}^- + \text{CH}_3\text{Cl}$	6.0	0.0	0.0
$\text{O}_2^{\bullet-} + \text{CH}_3\text{Cl}$	-5.9	-17.5	-17.6 ^c
$\text{SO}^{\bullet-} + \text{CH}_3\text{Cl}$	-6.8	-15.8	
$\text{OS}^{\bullet-} + \text{CH}_3\text{Cl}$	-1.2	-25.2	
$\text{S}_2^{\bullet-} + \text{CH}_3\text{Cl}$	4.4	-9.5	
$\text{HOS}^- + \text{CH}_3\text{Cl}$	-1.6	-29.3	
$\text{HS}^- + \text{CH}_3\text{Cl}$	0.3	-24.4	-22.0 \pm 2.4
$\text{HO}^- + \text{CH}_3\text{Cl}$	-12.8	-51.2	-49.7 \pm 0.1
$\text{HS}^- + \text{CH}_3\text{F}$	9.3	2.9	9.0 \pm 2.4
$\text{HO}^- + \text{CH}_3\text{F}$	-7.0	-23.8	-18.7 \pm 0.1

^a Classical energies calculated at MP4/6-31++G**//MP2/6-31++G** level. ΔE_{TS} is the difference in energy between the TS and the reactants. ΔE_{r} is the energy difference between products and reactants. $\Delta H_{\text{f}}(\text{expt})$ is the experimental enthalpy of reaction at 300 K for the $\text{S}_{\text{N}}2$ process. ^b Rate constants not included in Table 1: $k(\text{F}^- + \text{CH}_3\text{Cl}) = (1.41 \pm 0.01) \times 10^{-9} \text{ cm}^3 \text{ molecule}^{-1} \text{ s}^{-1}$, ref 17; $k(\text{Cl}^- + \text{CH}_3\text{Cl}) \approx 3.5 \times 10^{-14} \text{ cm}^3 \text{ molecule}^{-1} \text{ s}^{-1}$, see ref 53; $k(\text{HO}^- + \text{CH}_3\text{Cl}) = (1.80 \pm 0.04) \times 10^{-9} \text{ cm}^3 \text{ molecule}^{-1} \text{ s}^{-1}$, this paper; $k(\text{HS}^- + \text{CH}_3\text{F})$ no reaction; $k(\text{HO}^- + \text{CH}_3\text{F}) = 1.2 \times 10^{-11} \text{ cm}^3 \text{ molecule}^{-1} \text{ s}^{-1}$, ref 4. ^c The error could not be calculated due to the lack of error bars in the heat of formation of CH_3O_2 ,⁴⁶ $\Delta H_{\text{f}}(\text{CH}_3\text{O}_2) = 6.7 \text{ kcal mol}^{-1}$.

reacts 10 times faster (see Table 1). These results suggest that either the calculations at this level are inappropriate only for $\text{O}_2^{\bullet-}$ or that this anion is reacting through a different mechanism. The latter explanation seems more likely.

Since O_2 has an electron affinity (EA) of only 0.451 eV (10.4 kcal/mol),⁴⁰ much lower than for the other nucleophiles in this study (see Table 1), it seems reasonable to propose that electron transfer (ET) could play a role in this reaction, thus enhancing the $\text{O}_2^{\bullet-}$ reactivity with respect to other anions. Furthermore, this mechanism would give the same ionic product, making it experimentally indistinguishable from the $\text{S}_{\text{N}}2$ mechanism (eq 4).



For a given general reaction (eq 4), the $\text{S}_{\text{N}}2$ channel will always be more exothermic than the ET path since an additional bond is formed in the $\text{S}_{\text{N}}2$ pathway. On the other hand, as can be deduced from eq 4b, the ET process is also exothermic when the difference in EAs of Nu and the leaving group (X) is larger than the bond dissociation energy (BDE) in the neutral (eq 5a).

$$\text{EA}(\text{X}) - \text{EA}(\text{Nu}) > \text{BDE}(\text{CH}_3-\text{X}) \quad (5a)$$

An example of this process is the well-known dissociative electron capture reaction in methyl halides.⁴² Equation 5a can be rearranged to give

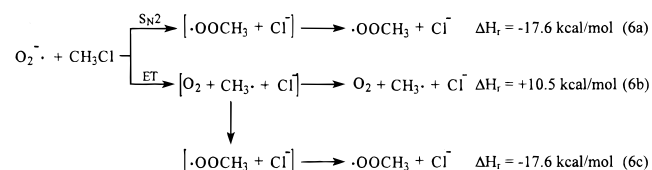
$$\text{EA}(\text{Nu}) < \text{EA}(\text{X}) - \text{BDE}(\text{CH}_3-\text{X}) \quad (5b)$$

which shows that a lower EA for Nu, a higher EA for the halogen atom, and smaller BDE for the carbon-halogen bond will favor an exothermic ET channel that could compete with the $\text{S}_{\text{N}}2$ process.

Recently, Shaik et al.^{8-10,43-45} have demonstrated theoretically that short-range ET reactions between radical anions and methyl

halides have well-structured transition states and that this mechanism is preferred kinetically over substitution in nucleophiles with small or even negative electron detachment energies. Nevertheless, for species with small EA values such as cyanoformaldehyde (EA ≈ -2 to 7 kcal/mol from data calculated by Shaik et al.⁹) a turnover from an $\text{S}_{\text{N}}2$ to an ET mechanism is observed in going from reaction of methyl chloride to methyl bromide to methyl iodide; for this series the right-hand side of eq 5b becomes larger (1.1 kcal/mol for X = Cl, 9.3 kcal/mol for X = Br, and 15 kcal/mol for X = I).⁴⁰ These results suggest that $\text{O}_2^{\bullet-}$, with an even higher adiabatic electron detachment energy than the cyanoformaldehyde radical anion, is expected to go through an $\text{S}_{\text{N}}2$ reaction mechanism with methyl chloride rather than through a short-range ET mechanism. Furthermore, both the ET and the $\text{S}_{\text{N}}2$ transition states seem to follow different reaction-specific orbital selection rules. This valence bond configuration mixing analysis suggests that the $\text{S}_{\text{N}}2$ and ET processes are two mutually exclusive mechanisms and that the lowest energy structure will occupy the saddle point, while the higher energy structure could be located at a higher order saddle point (not a TS).^{8,10} If this is true, the reaction $\text{O}_2^{\bullet-} + \text{CH}_3\text{Cl}$ will have a higher energy saddle point for the ET process than for the $\text{S}_{\text{N}}2$ channel or will not have a TS corresponding to ET at all. We have attempted to locate the ET-TS for this reaction (eq 6b) without success at the ROHF/6-31 G* level, a level that has proven to be adequate for this purpose.⁸

Equation 6 shows the experimental thermochemical values for the reaction of $\text{O}_2^{\bullet-}$ with CH_3Cl .^{40,46}



These values preclude the possibility of direct ET followed by dissociation to the products shown in eq 6b. However, an alternate mechanism is possible (eq 6c). Let us assume that the ET path can surmount the TS and reach the product ion-dipole complex $[\text{O}_2 + \text{CH}_3\cdot + \text{Cl}^-]$, which with about 15 kcal/mol stabilization¹⁰ would still have about 4 kcal/mol excess energy. Within this ion-dipole complex O_2 and the methyl radical could react to give the more stabilized $\text{S}_{\text{N}}2$ ion-dipole complex $[\text{CH}_3\text{OO}\cdot + \text{Cl}^-]$; this could subsequently dissociate to give the highly exothermic substitution products but through an ET process in a stepwise mechanism. The second step in this latter process (eq 6c) has been shown theoretically to possess a lower energy barrier than does the first step (ET) in similar systems.⁸

The question of the origin of the supernucleophilicity of $\text{O}_2^{\bullet-}$ still remains. Certainly, further inquiries into the mechanism of its reactions with alkyl halides are necessary to understand its reactivity. It is likely that reaction of $\text{O}_2^{\bullet-}$ with methyl chloride does not proceed through a classical $\text{S}_{\text{N}}2$ mechanism and that an ET process is probably favored,⁴⁷ although a direct ET with immediate dissociation as in 6b is thermodynamically forbidden. Tunneling effects in the ET mechanism or an alternate long-range ET mechanism could also play a role in enhancing the ET process; these mechanisms are not expected to contribute to the $\text{S}_{\text{N}}2$ pathway.

(42) Bertran, J.; Gallardo, I.; Moreno, M.; Saveant, J. M. *J. Am. Chem. Soc.* **1992**, *114*, 9576.

(43) Shaik, S.; Danovich, D.; Sastry, G. N.; Ayala, P. Y.; Schlegel, H. B. *J. Am. Chem. Soc.* **1997**, *119*, 9237-9245.

(44) Sastry, G. N.; Shaik, S. *J. Am. Chem. Soc.* **1998**, *120*, 2131-2145.

(45) Shaik, S.; Shurki, A. *Angew. Chem., Int. Ed. Engl.* **1999**, *38*, 587-625.

(46) Benson, S. W. *Thermochemical Kinetics*, 2nd ed.; Wiley-Interscience: New York, 1976.

(47) Marcus, R. A. *J. Phys. Chem. A* **1997**, *101*, 4072-4087.

Table 3. Comparison of Calculated Kinetic Isotope Effects for the S_N2 Reaction $Nu^- + CH_3Cl/CD_3Cl$ at 300 K, Using Different Methods^a

Nu ⁻	this work ^b							Truhlar et al. ^c							Westaway et al. ^d				exptl ^e η
	η_{trans}	η_{rot}	$\eta_{v,lo}$	$\eta_{v,mi}$	$\eta_{v,hi}$	η_{vib}	η	η_{trans}	η_{rot}	$\eta_{v,lo}$	$\eta_{v,mi}$	$\eta_{v,hi}$	η_{vib}	η	$\eta_{v,mi}$	$\eta_{v,hi}$	η_{vib}	η	
F ⁻	1.02	1.21	0.85	1.20	0.72	0.74	0.91								1.10	0.71	0.71	0.88	0.90 ± 0.02
Cl ⁻	1.04	1.22	0.85	1.33	0.69	0.78	0.99	1.04	1.22	0.85	1.26	0.71	0.76	0.95	1.18	0.68	0.74	0.94	1.2 ± 0.1^f
F ⁻ (H ₂ O)	1.04	1.63	0.62	1.14	0.72	0.51	0.86	1.04	1.66	0.61	1.07	0.74	0.48	0.83					0.85 ± 0.03
F ⁻ (H ₂ O/D ₂ O) ^g	1.05	1.34	0.75	1.20	0.51	0.46	0.65	1.05	1.35	0.74	1.14	0.55	0.46	0.65					0.65 ± 0.03

^a See the Experimental Section for the definitions of η , η_{trans} , η_{rot} , and η_{vib} . $\eta_{v,lo}$, $\eta_{v,mi}$, and $\eta_{v,hi}$ are the contributions to η_{vib} from low ($\nu < 600$ cm⁻¹), middle ($600 \leq \nu \leq 2000$ cm⁻¹) and high (>2000 cm⁻¹) frequency modes, respectively. ^b At MP2/6-31++G**//MP2/6-31++G** level and by using conventional TST. ^c Using a potential energy function based in results at the MP2/6-31G** level and improved canonical variational transition state theory (ICVT), corrected by using the centrifugal-dominant small-curvature semiclassical adiabatic ground state (CD-SCSAG) method to include tunneling, for Cl⁻.²⁰ For F⁻(H₂O) and F⁻(H₂O/D₂O), MP2/aug-cc-pVDZ//MP2/aug-cc-pVDZ was used together with conventional TST.¹⁶ ^d Conventional TST used with geometries and frequencies from HF/6-31+G* calculations.¹⁸ ^e From ref 17 unless otherwise stated. ^f From ref 48; see text for details in comparing this value with the others. ^g KIEs for F⁻(H₂O) + CH₃Cl vs F⁻(D₂O) + CH₃Cl.

Table 4. Calculated^a and Experimental Kinetic Isotope Effects

reaction	η_{low}	$\eta_{str,C-X}$	$\eta_{ben,out}$	$\eta_{ben,in}$	$\eta_{str,C-H}$	$\eta_{str,Nu}$	η_{vib}	η_{trans}	η_{rot}	η	KIE (exptl)	R_{TS}^b
F ⁻ + CH ₃ Cl	0.85	1.10	0.92	1.18	0.72		0.74	1.02	1.21	0.91	0.90 ± 0.02	4.14
Cl ⁻ + CH ₃ Cl	0.85	1.10	1.02	1.18	0.69		0.78	1.04	1.22	0.99		4.62
O ₂ ⁻ + CH ₃ Cl	0.66	1.08	0.87	1.20	0.80	1.00	0.59	1.03	1.56	0.95	0.91 ± 0.01	4.19
SO ₂ ⁻ + CH ₃ Cl	0.66	1.06	0.72	1.20	0.78	1.18	0.56	1.04	1.60	0.93		4.18
OS ₂ ⁻ + CH ₃ Cl	0.63	1.09	1.00	1.18	0.80	0.99	0.64	1.04	1.63	1.09	0.98 ± 0.02	4.65
S ₂ ⁻ + CH ₃ Cl	0.62	1.09	1.02	1.19	0.77	0.99	0.62	1.05	1.67	1.09		4.65
HOS ⁻ + CH ₃ Cl	0.63	1.07	1.01	1.18	0.76	0.99	0.60	1.04	1.65	1.03	0.96 ± 0.02 ^c	4.68
HS ⁻ + CH ₃ Cl	0.76	1.10	1.08	1.18	0.71	1.00	0.77	1.04	1.34	1.06	1.06 ± 0.03	4.71
HO ⁻ + CH ₃ Cl	0.75	1.10	0.98	1.18	0.74	1.00	0.70	1.02	1.27	0.91	0.93 ± 0.03 ^d	4.26
F ⁻ + CH ₃ F	0.84	1.14	0.83	1.24	0.74		0.73	1.05	1.23	0.94		3.66
Cl ⁻ + CH ₃ F	0.85	1.14	0.99	1.21	0.70		0.81	1.07	1.23	1.06		4.14
HS ⁻ + CH ₃ F	0.75	1.14	1.04	1.24	0.72	1.00	0.79	1.06	1.35	1.12		4.21
HO ⁻ + CH ₃ F	0.78	1.14	0.88	1.25	0.76	1.00	0.74	1.04	1.29	0.99		3.76

^a Frequencies calculated at MP2/6-31++G**//MP2/6-31++G** and using conventional transition state theory; see Experimental Section. See Experimental Section for a definition of frequencies included in each factor. ^b $R_{Nu-C} + R_{LG-C}$ in angstroms. ^c Possible contamination with the HSO⁻ isomer; see text for details. ^d $k(OH^- + CH_3Cl) = (1.80 \pm 0.04) \times 10^{-9}$ cm³ molecule⁻¹ s⁻¹, $k(OH^- + CD_3Cl) = (1.93 \pm 0.02) \times 10^{-9}$ cm³ molecule⁻¹ s⁻¹.

Kinetic Isotope Effects. Experimental KIE values for a variety of reactions have been used to rationalize their reaction mechanisms; in addition these values have been calculated with theoretical methods in order to understand the origin of the inverse secondary α -deuterium KIEs found in the S_N2 reaction mechanism.^{16,18–22,28} The usual interpretation of KIEs in terms of their correlation with the looseness of the TS recently generated considerable controversy.^{18,19,28} However, these KIEs can provide clues about the mechanism of the reaction of O₂⁻ with methyl chloride.

To test the theoretical results at the level used throughout this project, we calculated the KIEs for several S_N2 reactions that are well studied either experimentally or theoretically. The results are shown in Table 3, together with other theoretical and experimental values. The different contributions to the total η have been calculated as shown in eq 2, and further partitioning of η_{vib} was done to allow direct comparison with previously published values.

As can be seen, our total calculated KIEs (η) are in excellent agreement with experimental values.^{17,48} The experimental KIE for the reaction of Cl⁻ + CH₃Cl/CD₃Cl obtained by Ervin et al.⁴⁸ needs further discussion. These researchers used a guided ion beam instrument and reported an average KIE of 1.2 ± 0.1 for the entire energy window studied (0–4.5 eV). In fact, the extrapolated value at low energies (thermal energy) is more appropriate for comparison with flowing afterglow values as well as with our theoretical values. From Figure 12 of their paper⁴⁸ it is clear that the KIE falls to a value near 1.0 at low energies and that in this energy region the error bars increase to about 0.7. In addition, Table 3 shows that all individual

contributions to η for a given reaction are comparable among different authors, especially considering that they were calculated with completely different methods. We calculate normal, large normal, and inverse contributions from translation, rotation, and vibration factors, respectively; as has been shown before, the low- and high-frequency modes contribute to the inverse KIE, while a large normal contribution from the middle frequency modes brings the overall vibration factor closer to 1.

Probably the most computationally challenging reaction in Table 3 is the last one, F⁻(H₂O/D₂O) + CH₃Cl, which involves a solvent KIE, since there are very low-frequency modes in both reactants and TS. Nevertheless, our results are almost identical to the results obtained by Truhlar et al. at a higher level,¹⁶ except for a small difference in the mid- and high-frequency factors; these differences cancel out to give the same value for the total KIE, which is in good agreement with the experimental value. This agreement suggests that dynamic recrossing effects are negligible as well as that the computational level used in this paper is adequate for this purpose in this type of reaction.

Thus, we have calculated the KIEs for a set of 13 reactions involving O₂⁻ and other related nucleophiles. The results are presented in Table 4 including the detailed factoring of the vibrational contributions to the total η . With the exception of O₂⁻ and HOS⁻, there is very good agreement between the calculated total η and the experimental values taken from Table 1. The disagreement for O₂⁻ is not surprising on the basis of the discussion in the preceding section, but the disagreement for HOS⁻ is unexpected. Contamination with its isomer HSO⁻ (which, as discussed below, is expected to show a more inverse KIE) is improbable due to its method of synthesis, but we cannot rule out that some isomerization occurs at the SIFT injector. It is interesting to note that the experimental KIE for the reaction

(48) DeTuri, V. F.; Hintz, P. A.; Ervin, K. M. *J. Phys. Chem. A* **1997**, *101*, 5969.

of $\text{SO}^{\bullet-}$ with methyl chloride is intermediate between the calculated values for oxygen (inverse) and sulfur (normal) attack but much closer to the former; this suggests that oxygen attack is preferred, in agreement with the relative energies of the transition states shown in Table 2.

We will now analyze the changes in the KIEs from one reaction to another. The contributions to the η show the typical profile: slightly normal contribution from translations, large normal effects from rotations, and large inverse contributions from vibrations. Since the total KIEs in $\text{S}_{\text{N}}2$ reactions are usually inverse, this latter factor is generally recognized as the cause for these overall inverse effects. This is particularly true since vibrations are the *only* inverse contributions for all reactions considered in this study.

The translational contribution (η_{trans}) does not change appreciably and lies between 1.02 and 1.07 for all reactions studied. In contrast, the factor involving rotations clearly shows large variations among different reactions. This effect can be easily rationalized in terms of the changes in the moments of inertia produced upon deuteration of the corresponding hydrogen atoms and how they affect the η_{rot} . The moment of inertia (I) is related to the atom masses according to eq 7, where m_i are the

$$I = \sum_i m_i r_i^2 \quad (7)$$

atom masses and r_i are their perpendicular distances to the reference axis. The rotational partition function (Q_r) is directly related to the moments of inertia, according to eq 8, where I_A ,

$$Q_r = \frac{\pi^{1/2} (8\pi^2 k_{\text{B}} T)^{3/2} (I_A I_B I_C)^{1/2}}{\sigma h^3} \quad (8)$$

I_B , and I_C are the moments of inertia with respect to the three axes and σ is the symmetry number. According to transition state theory, η_{rot} is

$$\eta_{\text{rot}} = \frac{Q_r^{\text{H,TS}} / Q_r^{\text{H,R}}}{Q_r^{\text{D,TS}} / Q_r^{\text{D,R}}} \quad (9)$$

where superscripts indicate perprotio (H) or perdeuterio (D) labeled species and reactants (R) or transition state (TS), respectively. Equation 9 can be rearranged to

$$\eta_{\text{rot}} = \frac{Q_r^{\text{H,TS}}}{Q_r^{\text{D,TS}}} \cdot \frac{Q_r^{\text{D,R}}}{Q_r^{\text{H,R}}} \quad (10)$$

The numerical value of the second term in eq 10 will depend on the neutral molecule since contributions from the ion will cancel out; this value is 1.73 for methyl chloride. Thus, for different reactions with the same neutral, the final value for η_{rot} will be determined by *the ratio of the perprotio to the perdeuterio labeled rotational partition functions, evaluated at the transition states*. It follows that for a reaction involving a heavy nucleophile, the variation of the masses (m_i in eq 7) upon deuteration of the neutral will produce a smaller relative change in the moments of inertia than in a reaction with a lighter nucleophile. Thus, the first term in eq 10 becomes closer to unity for heavier nucleophiles, and since its value is smaller than 1 (because deuterium is heavier than hydrogen, eqs 8 and 10), it follows that *the final η_{rot} becomes larger for heavier nucleophiles reacting with the same neutral*. This is clearly seen in Table 4, for example, by comparing the η_{rot} for HO^- and HS^- with methyl chloride or methyl fluoride.

This mass effect is not the only one affecting η_{rot} as evident from the different η_{rot} values for $\text{OS}^{\bullet-}$ and $\text{SO}^{\bullet-}$ which have the same mass. In fact, as eq 7 shows, the spatial distribution of the different atoms (even when the total mass is the same) also plays a role in determining the value of the moments of inertia and η_{rot} ; by a similar argument as above for the masses, *a TS with more widely distributed atoms will produce a higher value for η_{rot}* . This effect will depend on the distribution of atoms in the TS and becomes more difficult to estimate a priori without knowledge of its structure.

In practice, both effects are important since we cannot modify the nucleophiles without changing the TS structure and vice versa, except by isotopic substitution. However, as Table 4 shows, it seems that the latter effect dominates and two groups of reactions emerge. The first group involves monatomic nucleophiles and diatomic nucleophiles containing a hydrogen atom (light atoms such as hydrogen make only small contributions to the moment of inertia) with η_{rot} values between 1.2 and 1.35; the second group contains di- and triatomic nucleophiles with at least two heavy atoms and has η_{rot} values around 1.6.

As mentioned before, the vibrational contribution is the only inverse factor, and since it also deviates most from unity, changes in the vibrational contribution will most significantly affect the final η value. Thus, η_{vib} was partitioned into contributions from different groups, each of them containing frequencies whose normal modes share some physical significance (see Experimental Section above). These contributions are also shown in Table 4.

Some groups of frequencies contribute with a constant factor for all reactions studied. This is the case for $\eta_{\text{str,C-X}}$, $\eta_{\text{str,Nu}}$, and $\eta_{\text{ben,in}}$. This is not surprising for $\eta_{\text{str,C-X}}$, since it is expected that the changes of this frequency upon deuteration in going from reactants to transition states do not change for reactions involving the same neutral. In addition, only a very slight variation is observed in going from the methyl chloride to the methyl fluoride series. A similar situation occurs for $\eta_{\text{str,Nu}}$ with the exception of the reaction of $\text{SO}^{\bullet-}$ with methyl chloride, where the S–O stretching frequency is surprisingly coupled with some H(D) motions in the transition state. The $\eta_{\text{ben,in}}$ factor, whose frequencies involve perpendicular movements of the H atoms with respect to the reaction coordinate, show very small changes when going from methyl chloride to methyl fluoride as a neutral. This feature and the fact that their contributions are normal (larger than 1) while η_{vib} are inverse (smaller than 1) suggest a minor contribution from these factors.

The other three factors are those that dominate and determine the inverse value for η_{vib} . The $\eta_{\text{str,C-H}}$ factor has inverse values for all the reactions studied and has been claimed to be the factor that governs η_{vib} and η in $\text{S}_{\text{N}}2$ reactions;^{19–22,28} however, other authors contend that the bending vibrations ($\eta_{\text{ben,out}}$ in this case) determine their magnitudes.¹⁸ As can be seen in Table 4, this latter factor ($\eta_{\text{ben,out}}$) changes substantially from one reaction to another having, in some cases, values larger than unity (normal contributions). This is a very interesting point to analyze. While $\eta_{\text{str,C-H}}$ values fluctuate only between 0.7 and 0.8, the $\eta_{\text{ben,out}}$ values are considerably more variable (between 0.72 and 1.08). The changes in the former have been correlated with the C–H bond strength or bond length in the transition states with respect to reactants^{19,28} while those of the latter have been associated with the transition state looseness.¹⁸ The transition state looseness (or tightness) is a simple idea that indicates how compressed a transition state is; however, this concept is difficult to quantify. There are two methods widely used to measure transition state looseness: the L and the R_{TS}

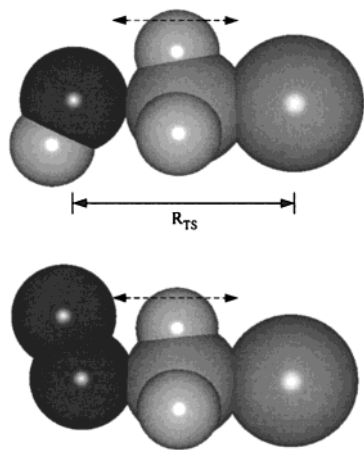


Figure 3. Structures of the transition states for the reactions of OH^- and $\text{O}_2^{\bullet-}$ with methyl chloride showing the space available for the α -hydrogen atoms bending vibrations and the R_{TS} parameter.

parameters. The former is the sum of the percent change of the carbon–nucleophile (C–Nu) and carbon leaving group (C–LG) bond lengths at the transition state with respect to products and reactants respectively (L^\ddagger) and with respect to the reactant and product complexes (L_{TS}).^{19,28} These methods give similar results. The latter is calculated by the sum of the C–Nu and C–LG bond lengths at the transition state;¹⁸ this approach seems more appropriate since it is related to the distance (“space”) available for the out-of-plane bending vibrations. These values are included in Table 4.

As evident in Table 4, there is a good correlation between $\eta_{\text{ben,out}}$ and the R_{TS} values for monatomic nucleophiles and diatomic nucleophiles with one hydrogen atom for either methyl fluoride or methyl chloride reactions, in agreement with previous reports.¹⁸ However, this correlation fails when considering polyatomic nucleophiles or even diatomic anions with two heavy atoms; this can be clearly seen by comparing, for example, $\text{O}_2^{\bullet-}$ and HO^- which have similar R_{TS} values but very different $\eta_{\text{ben,out}}$ contributions. We rationalize this fact by proposing that the change in the out-of-plane bending vibrations upon deuterating the TSs, with respect to the neutrals, depends on the actual *space* available for the α -hydrogens and that this *space* is not always proportional to the distance between nucleophile and leaving group. This idea is clearly depicted in Figure 3, which shows the TSs for the reactions of OH^- and $\text{O}_2^{\bullet-}$ with methyl chloride. Even when the R_{TS} values are comparable for these reactions, the *space* available for the α -hydrogens is clearly different, and this is observed in the different contributions from $\eta_{\text{ben,out}}$ for each reaction.

A similar and very interesting situation is observed for $\text{O}_2^{\bullet-}$ and $\text{SO}^{\bullet-}$. These TSs have the same R_{TS} value, but as can be anticipated, replacing an oxygen atom in $\text{O}_2^{\bullet-}$ with a much larger sulfur atom (see Figure 3) will decrease this *space* and further interfere with the out-of-plane bending vibrations; this causes a decrease (a more inverse) in its contribution to the KIE, in agreement with the results shown in Table 4. In light of these results it can also be anticipated that this effect will be less important at long Nu–C distances and become much more important at shorter distances where the atoms in the nucleophile are much closer to the α -hydrogens. This is clearly observed when comparing the $\eta_{\text{ben,out}}$ contribution for $\text{OS}^{\bullet-}$ and $\text{S}_2^{\bullet-}$ as nucleophiles. Since the S–C bond distance is significantly longer than the O–C distance by about 0.4 Å, replacing the oxygen atom by sulfur in this case does not change the $\eta_{\text{ben,out}}$ value.

Therefore, the R_{TS} (as well as the L) looseness parameters will not correlate with the $\eta_{\text{ben,out}}$ factor, unless we choose the appropriate nucleophiles (e.g., monatomic anions), but instead will correlate with the *crowdedness* of the transition state. A recent paper compares the different looseness parameters and identifies a new parameter, ΔR^\ddagger , that correlates well with the out-of-plane bending contributions to the KIEs.²⁹ ΔR^\ddagger include corrections for the nucleophile and leaving group atomic radius that will also affect the transition state crowdedness. Unfortunately, these authors included only three identity reactions involving monatomic nucleophiles. As we have shown, this parameter is also expected to fail in other cases, as in reactions of polyatomic nucleophiles.

In light of these results, the idea of transition state *crowdedness* should be used instead of the concept of *looseness*, particularly in systems where the attacking nucleophile has bulky atoms away from the reaction axis (facing toward the α -hydrogens) and in crowded systems. This is the case in substitution reactions occurring in proteins, where the looseness concept has been widely associated with α -H(D) secondary KIEs.^{24–27,49}

Finally, the η_{low} factor involves values that substantially deviate from unity. This factor is similar in importance to $\eta_{\text{str,C-H}}$ and $\eta_{\text{ben,out}}$ in determining the total η value. This feature has been discussed previously by Truhlar^{20,22,30,50,51} but has been overlooked by other authors mainly due to the improper grouping of frequencies where this effect remains hidden.^{18,19,28} There are three groups of reactions in Table 4, each of them showing a constant contribution. Clearly, it depends primarily on the type of nucleophile: monatomic nucleophiles with values of ~ 0.85 , diatomic nucleophiles with one hydrogen atom with values of ~ 0.76 , and diatomic or polyatomic nucleophiles with at least two heavy atoms with values of ~ 0.64 . This trend seems to follow the number of frequencies appearing in this group whose associated degrees of freedom in reactants correspond to rotations and translations; this depends on the number of atoms present in the nucleophile which determine the number of degrees of freedom. In addition each new frequency included in this group will contribute to a more inverse value because there is no associated frequency in the reactants (see eq 1). Therefore we recognized that this behavior may be an artifact and that if we include the associated degrees of freedom in the same group, these effects could be canceled. Effectively, if we define a new group obtained by multiplying the values obtained for η_{low} , η_{trans} , and η_{rot} , which will have a correlated and constant number of degrees of freedom, we obtain a constant value of 1.07 ± 0.03 .⁵²

These results lead us to conclude that KIEs in the $\text{S}_{\text{N}}2$ reactions are mainly determined by the $\eta_{\text{ben,out}}$ contribution and that this factor depends on the *crowdedness* of the transition state for a given neutral, in accord with the accepted empirical rule. We restate this idea in light of our new results: for a particular substrate, a highly crowded transition state (as defined above) will have a smaller α secondary KIE value than a less crowded transition state.

Conclusions

The enhanced reactivity of $\text{O}_2^{\bullet-}$ with alkyl halides has been confirmed in comparison with anions and radical anions of

(49) Williams, I. H. *J. Am. Chem. Soc.* **1984**, *106*, 7206–12.

(50) Truhlar, D. G.; Lu, D. H.; Tucker, S. C.; Zhao, X. G.; Gonzalez-Lafont, A.; Truong, T. N.; Maurice, D.; Liu, Y. P.; Lynch, G. C. *ACS Symp. Ser.* **1992**, No. 502, 16–36.

(51) Hu, W.-P.; Truhlar, D. G. *J. Am. Chem. Soc.* **1996**, *118*, 860–9.

(52) The reported error bars correspond to one standard deviation.

(53) Barlow, S. E.; Van Doren, J. M.; Bierbaum, V. M. *J. Am. Chem. Soc.* **1988**, *110*, 7240.

similar basicity. Potential energy surface calculations and experimental and theoretical KIEs suggest that this anion is not reacting by a classical S_N2 mechanism. A simple ET process is not thermodynamically allowed, but ET followed by radical-radical coupling in the product well is possible; this process will generate the same products as the S_N2 reaction in a stepwise mechanism. However, we are unable to locate a structured ET-TS as suggested by Shaik and co-workers;⁸⁻¹⁰ moreover their VBCM analysis excludes the existence of this structure as a first order saddle point, suggesting that a long-range (weakly bonded) ET process may occur in this system.

We have performed an exhaustive analysis of the secondary α -deuterium KIEs in the S_N2 mechanism including mono- and polyatomic nucleophiles. The agreement between experimental and theoretical results is extremely good and factoring of the different contributions leads to the following conclusions: (1) Total KIEs are not always inverse (<1) as has been assumed in the past; therefore assigning the effect to a single factor because its contribution is inverse (as $\eta_{str,C-H}$) is not necessarily correct. (2) η_{low} is, in general, one of the most inverse factors; however the product $\eta_{low}\eta_{trans}\eta_{rot}$ that includes a constant number of degrees of freedom and a correspondence between them

shows a constant slightly normal contribution. (3) $\eta_{str,C-H}$ and $\eta_{ben,in}$ reveal almost constant values with small changes for different leaving groups. Also $\eta_{str,Nu}$ show constant values except for the reaction of $SO^{\bullet-}$ with methyl chloride. (4) Although the total KIE is determined by both $\eta_{str,C-H}$ and $\eta_{ben,out}$, the contribution from the $\eta_{str,C-H}$ factor does not change significantly compared with $\eta_{ben,out}$ for all the reactions studied. This latter component, on the other hand, changes markedly from one reaction to another. Thus, the magnitude of the total KIE is primarily determined by $\eta_{ben,out}$ and the accepted empirical relationship between the secondary α -deuterium KIEs and the $\alpha C-H(D)$ out-of-plane bending vibrations is basically correct. (5) $\eta_{ben,out}$, which largely determines the magnitude of the total KIE for a particular neutral, is related to the transition state *crowdedness* and not to the usual *looseness* (or *tightness*) interpretation.

Acknowledgment. We gratefully acknowledge support of this research by the National Science Foundation under Grant No. CHE-9734867. We appreciate the helpful comments of the reviewers.

JA993093X